


Identification of Siglec-10 as a new dendritic cell checkpoint for cervical cancer immunotherapy

Congwen Wang,^{1,2} Lewei He,^{1,2} Jing Peng,^{1,2} Chong Lu,^{1,2} Meng Zhang,^{1,2} Xingling Qi,^{1,2} Mingxing Zhang,^{1,2} Yumeng Wang ^{2,3}

To cite: Wang C, He L, Peng J, *et al.* Identification of Siglec-10 as a new dendritic cell checkpoint for cervical cancer immunotherapy. *Journal for ImmunoTherapy of Cancer* 2024;**12**:e009404. doi:10.1136/jitc-2024-009404

► Additional supplemental material is published online only. To view, please visit the journal online (<https://doi.org/10.1136/jitc-2024-009404>).

CW and LH contributed equally.

Accepted 14 August 2024



© Author(s) (or their employer(s)) 2024. Re-use permitted under CC BY-NC. No commercial re-use. See rights and permissions. Published by BMJ.

¹Department of Integration of Western and Traditional Medicine, Obstetrics and Gynecology Hospital of Fudan University, Shanghai, People's Republic of China

²Shanghai Key Laboratory of Female Reproductive Endocrine Related Diseases, Obstetrics and Gynecology Hospital of Fudan University, Shanghai, People's Republic of China

³Department of Gynecology, Obstetrics and Gynecology Hospital of Fudan University, Shanghai, People's Republic of China

Correspondence to

Dr Yumeng Wang;
20111250016@fudan.edu.cn

Dr Mingxing Zhang;
zhangmingxing_2008@yeah.net

ABSTRACT

Background The occurrence of chronic inflammation resulting from infection with human papillomaviruses is an important factor in the development of cervical cancer (CC); thus, deciphering the crosstalk between the tumor microenvironment and innate immune cells during the establishment of immune tolerance is vital for identifying potential treatment strategies.

Methods Single-cell RNA sequencing data and primary tumor samples from patients with CC were used to evaluate the functional role of Siglec-10 on dendritic cells (DCs). Patient-derived tumor fragment platforms were used to examine the ability of Siglec-10 blockade to reinvigorate DC-mediated T-cell activation and tumor clearance.

Results Here, we demonstrated that Siglec-10 is a prominent inhibitory checkpoint for DCs infiltrated in CC. CC epithelial cells use their aberrant surface sialylated structures to induce the transformation of conventional DCs into phenotypes characterized by low immunogenicity and high immunotolerance. Additionally, Siglec-10⁺ DCs suppress the function of adaptive T cells via galectin-9 signaling to strengthen the immunosuppressive CC microenvironment. Disturbance of Siglec-10 signaling restored the DC-mediated tumoricidal response and increased adaptive T cells sensitivity to programmed cell death protein 1 inhibition.

Conclusion Our study confirms the checkpoint role of Siglec-10 on DCs and proposes that targeting Siglec-10 may be a promising avenue for immunotherapy against CC.

INTRODUCTION

Cervical cancer (CC) is a prominent cause of mortality among women worldwide that is primarily caused by oncogenic human papillomaviruses (HPVs).¹ Extensive evidence has demonstrated that the strength of the local immune response plays a pivotal role in determining the outcome of HPV infections, leading to either neoplasia or complete eradication.^{2–3} Dendritic cells (DCs), which serve as the primary defense against tumors, have been observed to accumulate in the peritumoral and tumorous regions in CC and other cancers.^{4–8} Despite the substantial influx of

WHAT IS ALREADY KNOWN ON THIS TOPIC

⇒ Prior scientific understandings have highlighted the pivotal role of dendritic cells (DCs) in modulating tumor immunity, yet gaps persisted in elucidating their functional regulation in cervical cancer, necessitating this study to bridge the knowledge divide.

WHAT THIS STUDY ADDS

⇒ This study highlights the potential role of the sialoglycan/Siglec-10 axis, in modulating DC mediated-immunosuppression in cervical cancer.

HOW THIS STUDY MIGHT AFFECT RESEARCH, PRACTICE OR POLICY

⇒ Understanding the mechanisms of Siglec-10-mediated immunosuppression in cervical cancer may lead to the development of novel treatment strategies for improving patient outcomes.

DCs into tumors, their ability to exert a robust adaptive antitumor immune response is often limited. Tumor-infiltrated DCs are susceptible to tumor/regulatory T cells (Treg)-secreted immune suppressors (interleukin (IL)-10, vascular endothelial growth factor (VEGF), transforming growth factor (TGF)- β , prostaglandin E2 (PGE2), etc),⁹ and immunoregulatory signals in the TME, including RANKL, PD-Ls, and IDO-1.^{10–12} These factors compromise the function of DCs or repolarize mature DCs into tolerogenic DCs, which induce T-cell anergy and apoptosis to counter effective immune killing.^{12–13} This interplay between CC and DCs has presented a considerable challenge in immunotherapy strategies that aim to target effector immune cells, potentially providing an explanation for the failure of immunotherapeutic interventions observed among specific patients. Further dissection of the diverse phenotypes of DCs within the CC microenvironment could offer important insights for immune response modulation and effective therapeutic intervention in CC.

In recent years, numerous studies have indicated the potential of the sialoglycan-sialic acid-binding immunoglobulin-like lectin (Siglec) axis within the TME as a novel immune checkpoint that drives innate and adaptive antitumor immunity.¹⁴ The inhibitory Siglec receptors possess structural and signaling motifs that are similar to those of the widely recognized inhibitory receptor programmed cell death protein-1 (PD-1); these motifs include an immunoreceptor tyrosine-based inhibitory motif (ITIM) and an ITIM-like motif that can regulate intracellular signaling by interacting with SHP1 and SHP2 phosphatases.¹⁵ The primary physiological function of most inhibitory Siglec receptors is to act as immune checkpoints, thereby preventing undesired immune responses.¹⁶ In the context of cancer, aberrant glycosylation, a frequently observed characteristic, is exploited by tumor cells to establish an immunosuppressive environment and facilitate disease progression.¹⁷ A recent study provided evidence for interactions between sialoglycan ligands and Siglec receptors within the TME, specifically in relation to tumor-associated macrophages.¹⁴ Although the various functions of Siglecs in multiple immune cells are becoming increasingly understood, there is still limited evidence supporting a connection between Siglecs and the functional heterogeneity of DCs, particularly in the specific context of cancer. In the CC microenvironment, the effect of Siglec expression in DCs in terms of specific functional outcomes has not yet been determined.

To interrogate these questions, we searched single-cell and bulk RNA sequencing databases as well as enrolled CC cohorts to ultimately identify Siglec-10 as the predominant Siglecs in CC, which is closely linked to the function of DCs and disease prognosis. The hypersialoglycans in CC tumor epithelial cells induce the tolerogenic transformation of Siglec-10⁺ DCs, leading to T-cell exhaustion and facilitating tumor immune evasion. Using patient-derived tumor fragment (PDTF) platforms in our investigations, we proposed an approach that targets Siglec-10 and prevents the immunosuppressive effects mediated by Siglec-10⁺ DCs in the context of CC immunotherapy.

RESULTS

The expression of Siglec-10 in CC-infiltrated DCs predicts patient prognosis

To explore the role of the Siglec family in the CC microenvironment, we performed single-cell RNA sequencing (scRNA-seq) analysis on publicly available data sets, including nine cervical tumor tissue (TT) and four adjacent normal tissue (NT) samples.^{18,19} Cells were clustered using a graph-based shared nearest neighbor approach followed by t-distributed stochastic neighbor embedding (t-SNE) dimension reduction, which yielded 11 known cell types (online supplemental figure S1). A total of 743 DCs including 646 CC-infiltrated DCs and 73 NT-infiltrated DCs were obtained for further analysis. To identify the potential functional molecules of CC-infiltrated DCs,

the expression of all 14 members of the Siglec family was analyzed in TT and NT cells. As shown in [figure 1A](#), low expression of Siglec-2, Siglec-7, Siglec-9, Siglec-12, and Siglec-14; moderate expression of Siglec-1, Siglec-3, and Siglec-10; and high expression of the Siglec-10 gene was observed in CC-infiltrated DCs, while extremely low expression of the remaining Siglecs was found. The expression levels of all Siglecs remained low in DCs from NTs. In addition to DCs, Siglecs were shown to be distributed on B cells and other myeloid cells (online supplemental figure S2A). Next, to determine which Siglecs expressed by DCs influence the survival of patients with CC, we analyzed data from The Cancer Genome Atlas Program (TCGA) cervical squamous cell carcinoma (CESC) cohort, particularly focusing on patients with abundant tumor-infiltrating DCs (estimated by CIBERSORT). Using the cell signatures for different Siglec-expressing DCs derived from the scRNA-seq data (online supplemental table S1), overall survival was compared between samples stratified by the median signature score. We found that the Siglec-10⁺ signature score was an unfavorable prognostic factor in patients with CC (HR=0.4763, 95% CI=0.2362 to 0.9605, p=0.03); however, there were no statistically significant differences between the high-groups and low-groups stratified by other Siglecs⁺ DC scores ([figure 1B](#)). The Siglec-10⁺ signature in the CC TME could efficiently discriminate between patients with good or poor prognosis ([figure 1C](#)). These results suggested that Siglec-10, but not other Siglecs, may play a role in shaping the TME of CC.

Elevated infiltration of Siglec-10⁺ DCs correlates with late clinical stage and increased recurrence risk in patients with CC

To confirm the clinical significance of Siglec-10 expression by DCs, we evaluated the infiltration of Siglec-10⁺ DCs in our independent CC cohort. Consistent with the results of the scRNA-seq analysis, the flow cytometry results showed significantly upregulated Siglec-10 expression in CC-infiltrated DCs compared with NT-infiltrated DCs (online supplemental figure S2B). Multiplex immunofluorescence staining further highlighted the abundance of Siglec-10⁺ DCs in the intratumoral area, while both DCs and Siglec-10 were scarce in the adjacent NT area ([figure 1D](#)). A greater percentage of CC-infiltrated DCs with Siglec-10 expression was observed in tumors with larger diameters and later International Federation of Gynecology and Obstetrics stages. Additionally, in patients who possessed high-risk factors for early recurrence and poor prognosis, such as lymph node metastasis, lymphovascular invasion, and deep stromal invasion, more intratumoral infiltration of Siglec-10⁺ DCs was observed ([figure 1E](#) and online supplemental table S2). These data suggested that intratumoral Siglec-10⁺ DCs play a protumorigenic role in CC.

Siglec-10 is widely expressed in diverse conventional dendritic cell subpopulations but not in plasmacytoid dendritic cells in CC tumors

scRNA-seq data of DCs derived from CC tumor specimens were obtained to further characterize Siglec-10⁺

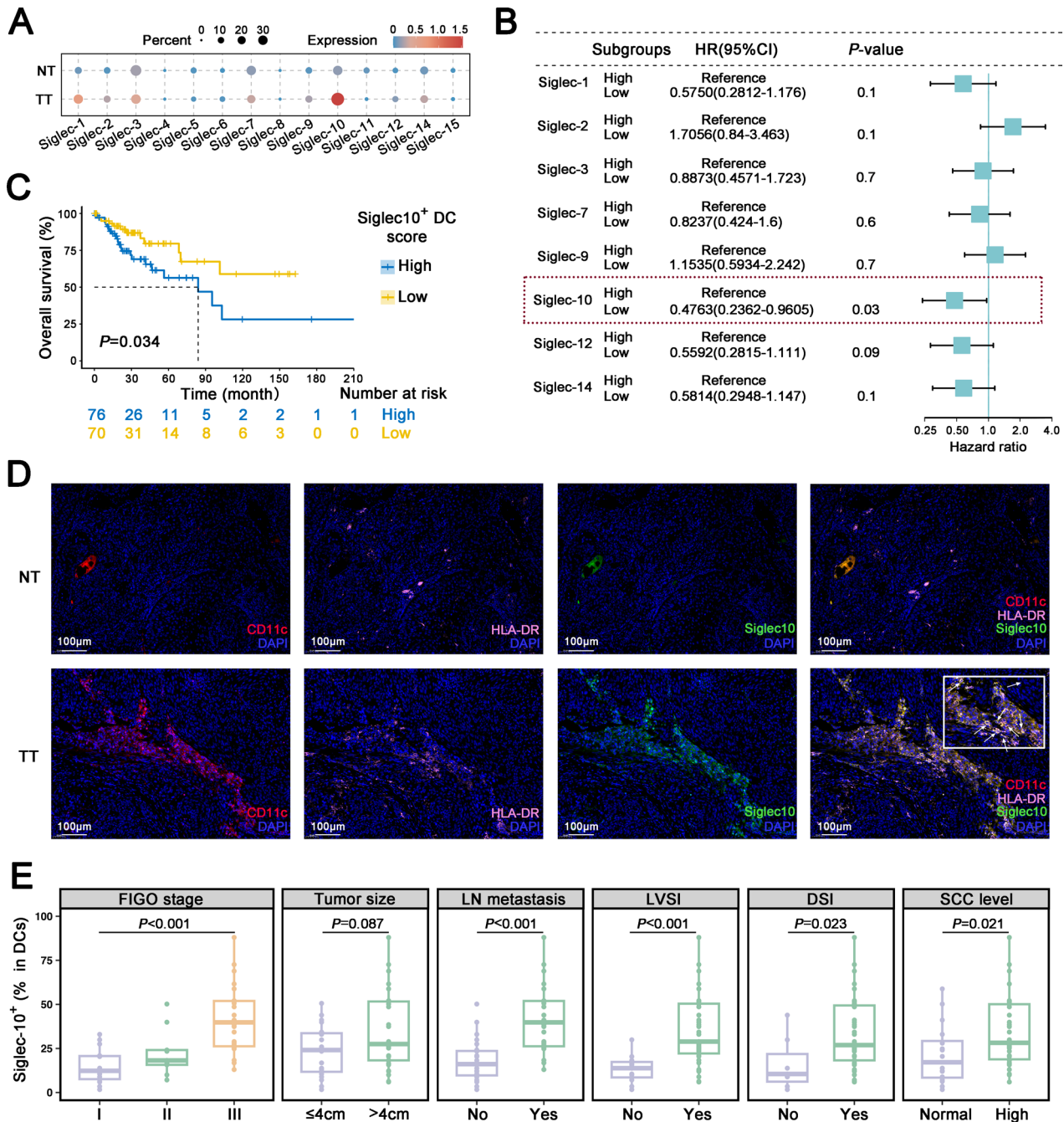


Figure 1 The upregulated expression of Siglec-10 in infiltrated DCs was correlated with poor prognosis and worse disease conditions in patients with cervical cancer. (A) Bubble heatmap showing the gene expression of Siglec family members among DCs across the NT and TT samples. (B) Cox regression univariate analysis of TCGA CESC patients (n=291) based on the gene signature expression of Siglec⁺ DCs. The significance of the covariates was calculated by the Wald test. (C) The Kaplan-Meier overall survival curve of TCGA CESC patients (n=291) grouped according to the gene signature expression of Siglec-10⁺ DCs. Significance was calculated by the log-rank test. (D) Representative multicolor immunofluorescence staining of CD11c⁺HLA-DR⁺Siglec-10⁺ cells that infiltrated the NT or TT samples. (E) Percentages of Siglec-10⁺ cells within tumor-infiltrated DCs in patients with different clinicopathological parameters, as determined via flow cytometry analysis (n=50). Significance was calculated by the Mann-Whitney U test (two groups) or the Kruskal-Wallis test (multiple groups). CESC, cervical squamous cell carcinoma; DCs, dendritic cells; DSI, deep stromal invasion; LN, lymph node; LVSI, lymphovascular invasion; SCC, NT, normal tissue; SCC, squamous cell carcinoma antigen; TCGA, the Cancer Genome Atlas Program; TT, tumor tissue.

DCs. Unsupervised clustering identified three subsets of conventional dendritic cells (cDCs) (cDC1s, cDC2s, and recently reported LAMP3⁺ DCs) and a subset of plasmacytoid dendritic cells (pDCs) (figure 2A).²⁰ Intriguingly,

we found that Siglec-10 gene was extensively detected in three cDC subsets, but was largely absent in the pDC subset (figure 2B). Flow cytometry analysis of 24 TT specimens was used to further elucidate the distribution

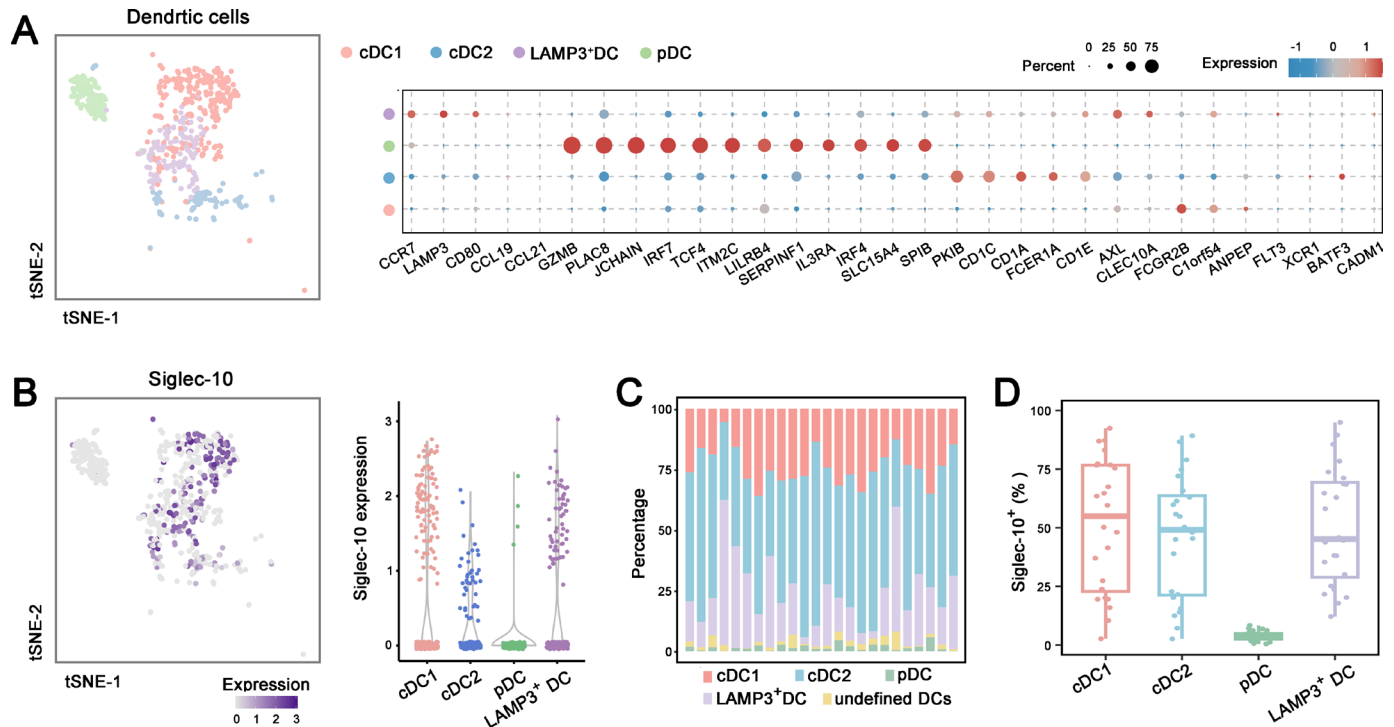


Figure 2 Distribution characteristics of cervical cancer-infiltrated Siglec-10⁺ DCs. (A) t-SNE plot showing the four subtypes of DC clusters derived from TT samples. Bubble heatmap showing marker genes across four DC clusters derived from TT samples. (B) t-SNE plot and violin plot showing the expression level of Siglec-10 among different DC subpopulations. (C) Subpopulation distribution of Siglec-10⁺ DCs in each TT sample. (D) Expression of Siglec-10 in four DC clusters determined via flow cytometry analysis (n=24). cDC, conventional DC; DC, dendritic cells; pDC, plasmacytoid dendritic cells; t-SNE, t-distributed stochastic neighbor embedding; TT, tumor tissue.

of the Siglec-10 protein in distinct DC subsets (online supplemental figure S2C). We confirmed that Siglec-10-expressing DCs were overwhelmingly cDCs despite the significant heterogeneity in the proportion of Siglec-10-expressing DCs in each subset (figure 2C,D). Minimal levels of the Siglec-10 protein were detected on the surface of pDCs.

Siglec-10 expression defines an immunoregulatory CC-infiltrated DC phenotype

We next performed monocle analysis to explore the distribution of Siglec-10⁺ DCs along the inferred DC trajectory. The constructed trajectory of intratumoral DCs revealed two different branches, and Siglec-10 was mainly distributed in the cell fate one branch (figure 3A). To investigate the functional status during cell-state transitions, gene module scores for each cell based on predefined “activated” and “tolerogenic” associated gene sets were calculated.^{21–23} DCs at the starting point of the pseudotime presented enrichment of activation score, while DCs directed to cell fate one exhibited a decrease in the tolerogenic score and an increase in the activation score (figure 3B). This tolerogenic transformation of DCs was accompanied by consistent upregulation of Siglec-10 expression, indicating the potential role of Siglec-10 in promoting DC tolerance in CC.

To further elucidate the phenotype of Siglec-10-expressing DCs, a Gene Set Enrichment Analysis

was conducted to determine the enriched pathways. Compared with Siglec-10⁻ DCs, Siglec-10⁺ DCs were enriched in the antigen processing and presentation pathway and had higher expression of HLA molecules and antigen recognition/processing molecules (CTSA, CTSC, TAP2, and FCGR3A) (figure 3C,D). By tracking fluorescein 5-isothiocyanate (FITC)-dextran engulfment by tumor-sorted DCs ex vivo, the phagocytic ability of Siglec-10⁺ DCs was confirmed to be greater than that of Siglec-10⁻ DCs (figure 3E). As indicated by the scRNA-seq data, there was an imbalance between stimulatory and immunoregulatory signals in Siglec-10⁺ DCs, as indicated by the significant downregulation of CD83 and upregulation of inhibitory molecules such as HAVCR2, SLAMF7, CD163, and LILRBs (figure 3D). In addition, pathways related to adaptive immune function including the CD40 pathway, the chemokine pathway, cytokine signaling and JAK/STAT signaling, were negatively enriched in the Siglec-10⁺ DCs (figure 3C). The phenotype of Siglec-10⁺ DCs was further elucidated by a comprehensive flow cytometry analysis of our CC cohort using classical markers related to DC function (figure 3F and online supplemental figure S3). Significant downregulation of the costimulatory markers CD40, CD80, CD83 and CD86 were observed in the Siglec-10⁺ DCs, while the inhibitory ligand programmed death-ligand 1 (PD-L1) was upregulated. Two inhibitory receptors, PD-1 and Tim-3, which

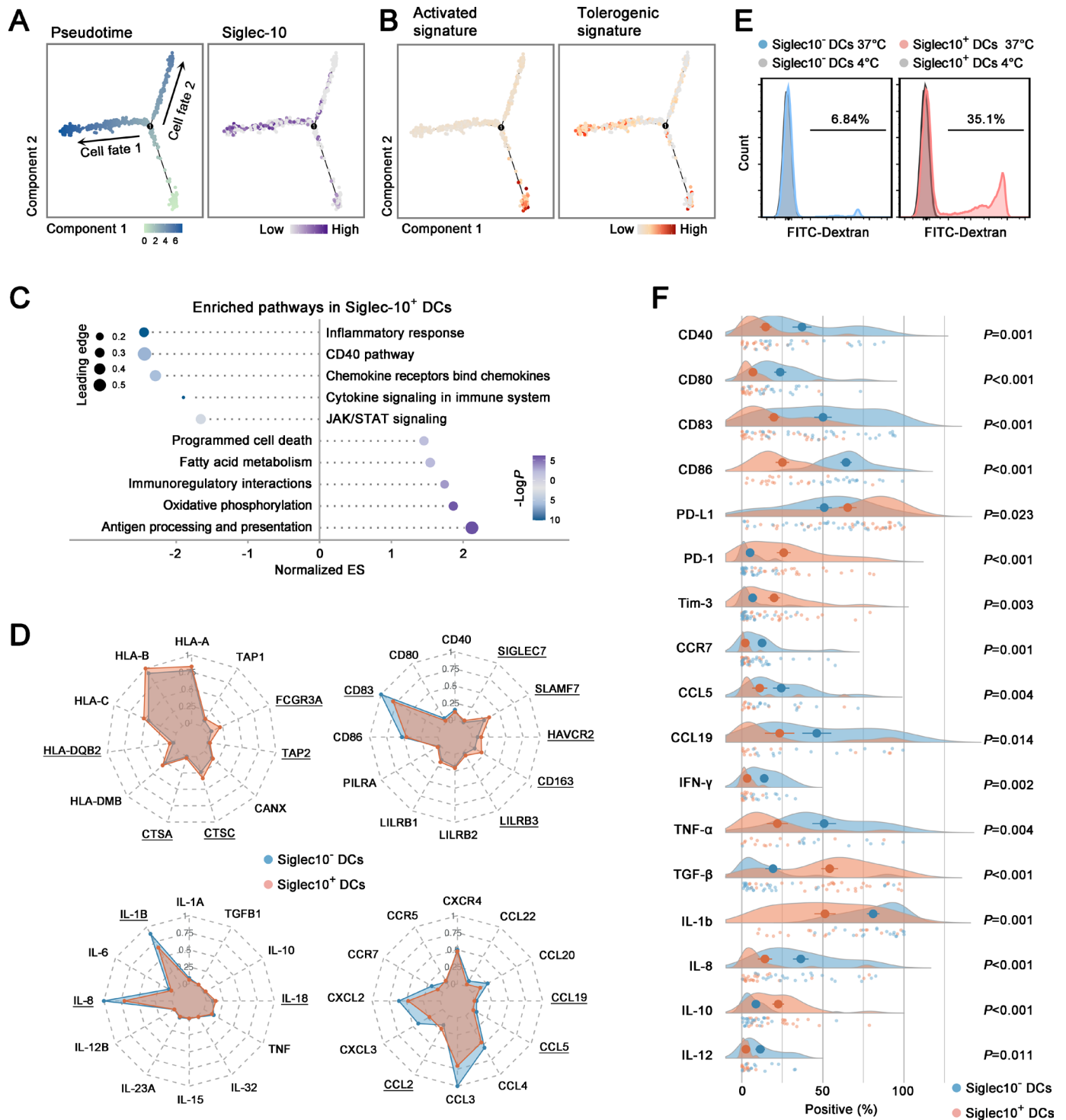


Figure 3 Tolerogenic phenotype of cervical cancer-infiltrated Siglec-10⁺ DCs. (A) Trajectory inference analysis and dynamic changes in Siglec-10 expression on DCs from TTs. (B) Pseudotime projections showing the activated or tolerogenic signatures. (C) Two-sided bar graph showing the pathways associated with significantly upregulated and downregulated genes in Siglec-10⁺ DCs in TTs according to Gene Set Enrichment Analysis. (D) Radar plots showing the immunogram patterns of Siglec-10⁺ DCs and Siglec-10⁻ DCs. Underlined labels indicate significant differences (p < 0.05). Significance was calculated by the Wilcoxon test. (E) Representative histograms showing the endocytosis of FITC-dextran in Siglec-10⁻ DCs and Siglec-10⁺ DCs. (F) Raincloud plots indicating the positive expression of designated markers in tumor-infiltrated Siglec-10⁺ DCs or Siglec-10⁻ DCs based on flow cytometry analysis (n=14–31). Significance was calculated by the Mann-Whitney U test. DC, dendritic cell; ES, enrichment score; FITC, fluorescein 5-isothiocyanate; TT, tumor tissue.

are reported to negatively regulate the immunogenic function of DCs, were highly expressed on Siglec-10⁺ DCs compared with Siglec-10⁻ DCs.^{24 25} Similarly, Siglec-10⁺ DCs almost completely lost CCR7 expression and exhibited decreased secretion of CCL5 and CCL19, indicating defects in chemotactic movement and the chemotaxis of other immune cells. In contrast to Siglec-10⁻ DCs, Siglec-10⁺ DCs tended to produce more anti-inflammatory cytokines while preventing proinflammatory cytokines, suggesting that Siglec-10⁺ DCs are deficient in mediating the antitumor response. Specifically, we found specific enrichment of oxidative phosphorylation and fatty acid metabolism in Siglec-10⁺ DCs (figure 3C), which reportedly support the maintenance of the immunosuppressive phenotype of tolerogenic DCs.^{13 26}

Enhanced sialylation/Siglec-10 interactions in CC promotes the repolarization of DCs to the immunoregulatory DC phenotype

Hypersialylation has been described as a hallmark of multiple cancers and can be recognized by Siglecs to trigger immunomodulatory programs in macrophages, T cells and natural killer cells. However, little is known about how sialic acid signals are involved in Siglec-10-mediated functional changes in DC within the CC environment. To assess whether more active sialylation occurs in the CC environment, the expression of key enzyme components of the sialylation machinery was evaluated using scRNA-seq data. Compared with the epithelial cells in NT, the epithelial cells in TT showed upregulated expression of GNE, NANS, NANP, and CMAS, suggesting a general increase of sialic acid-donor syntheses pathway in CC (figure 4A). The Siglec-10 ligand signals in the NT and TT regions of the CC environment were investigated using a recombinant human Siglec-10 hFc chimera. Quantification of the signal intensity revealed a significant increase in sialylation in tumor regions compared with adjacent normal regions (figure 4B,C). Next, we explored the correlation between sialylation scores and immune infiltration in the TCGA CSEC cohort. In agreement with previous studies reporting the inhibitory effect of the Siglec-10 pathway on macrophages, the intensity of the sialylation signals was strongly negatively correlated with macrophages and monocytes. Strikingly, despite no correlation between sialylation signals and myeloid DC infiltration, a considerably low proportion of activated DCs was correlated with higher sialylation levels. Moreover, the sialylation scores were positively correlated with the regulatory genes of DCs but negatively correlated with genes associated with immunogenic stimulation (figure 4D).

Next, we sought to assess the functional implications of the interaction between Siglec-10 and its ligands on DCs. The expression intensity of Siglec-10 ligands was measured in a total of 7 CC cell lines (HeLa, CaSki, C-33A, SiHa, ME180, MS751 and SW756) by flow cytometry. SW756 and SiHa cells exhibited the strongest surface Siglec-10 ligand signals and were chosen for the subsequent

experiments (online supplemental figure S4A,B). The binding of Siglec-10 hFc signals to Siglec-10 was abrogated by neuraminidase, which digests sialylated structures,²⁷ thus confirming the positive expression of Siglec-10 ligands on tumor cells (online supplemental figure S4C). On stimulation by CC cells, Siglec-10⁺ DCs released more tumor-promoting factors (IL-10 and TGF- β) but fewer activation signals (CD40, CD83, and CD86) and tumor suppressors (IL-1b, IL-12, and CCL19) after binding to Siglec-10 ligands (figure 4E,F). Following enzymatic digestion of Siglec-10 ligands, only Siglec-10⁺ DCs exhibited enhanced functional activation and an altered cytokine synthesis profile (figure 4E,F), indicating that this peculiar phenotype of Siglec-10⁺ DCs is determined by the stimulation received from sialylation signals. Collectively, these results demonstrate that the aberrant upregulation of sialylation/Siglec-10 interactions within CC foci leads to the suppressive functional transformation of DCs to support tumor growth.

Enrichment of Siglec-10⁺ DCs contributes to CC immune evasion by compromising antitumor T-cell function

To further probe the role of this distinct Siglec-10⁺ DC subset in shaping the CC immune microenvironment, we profiled the differentially expressed genes (DEGs) between the high-Siglec-10⁺ and low-Siglec-10⁺ DC infiltration groups in the TCGA CESC cohort (online supplemental table S3). The expression of inflammatory factors was examined, revealing increased levels of the protumorigenic factor IL-10 and decreased levels of the anti-tumor IL-12 in the TME with elevated Siglec-10⁺ DC infiltration (online supplemental figure S5A). The results of Gene Ontology annotation and enrichment analysis revealed significant enrichment of multiple immunosuppressive signals in the population with increased Siglec-10⁺ DC infiltration (figure 5A). The above results indicated that Siglec-10⁺ DCs act as mediators of immune escape in the CC microenvironment. We next inferred intercellular communications between different DC subsets and other cell types using the CellChat algorithm (figure 5B). Epithelial cells were predicted to be the dominant cell type receiving ligand signaling from DCs. Notably, T cells were detected to receive stronger outgoing interaction signals originating from Siglec-10⁺ DCs than from Siglec-10⁻ DCs, suggesting that T cells might be the prominent downstream population regulated by Siglec-10⁺ DCs.

To determine the degree of tumor immune escape in patients with abundant Siglec-10⁺ DCs in their TME, the tumor immune dysfunction and exclusion score of the CESC cohort was calculated. The samples with increased Siglec-10⁺ DC infiltration presented a decreased T-cell exclusion signature but an increased T-cell dysfunction signature (figure 5C). Further estimations of immune infiltration levels by six estimation algorithms indicated a significant positive correlation between the Siglec-10⁺ DC score and CD8⁺ T-cell infiltration, with excellent agreement between the different estimation models (figure 5D and online supplemental figure S5B). The number of

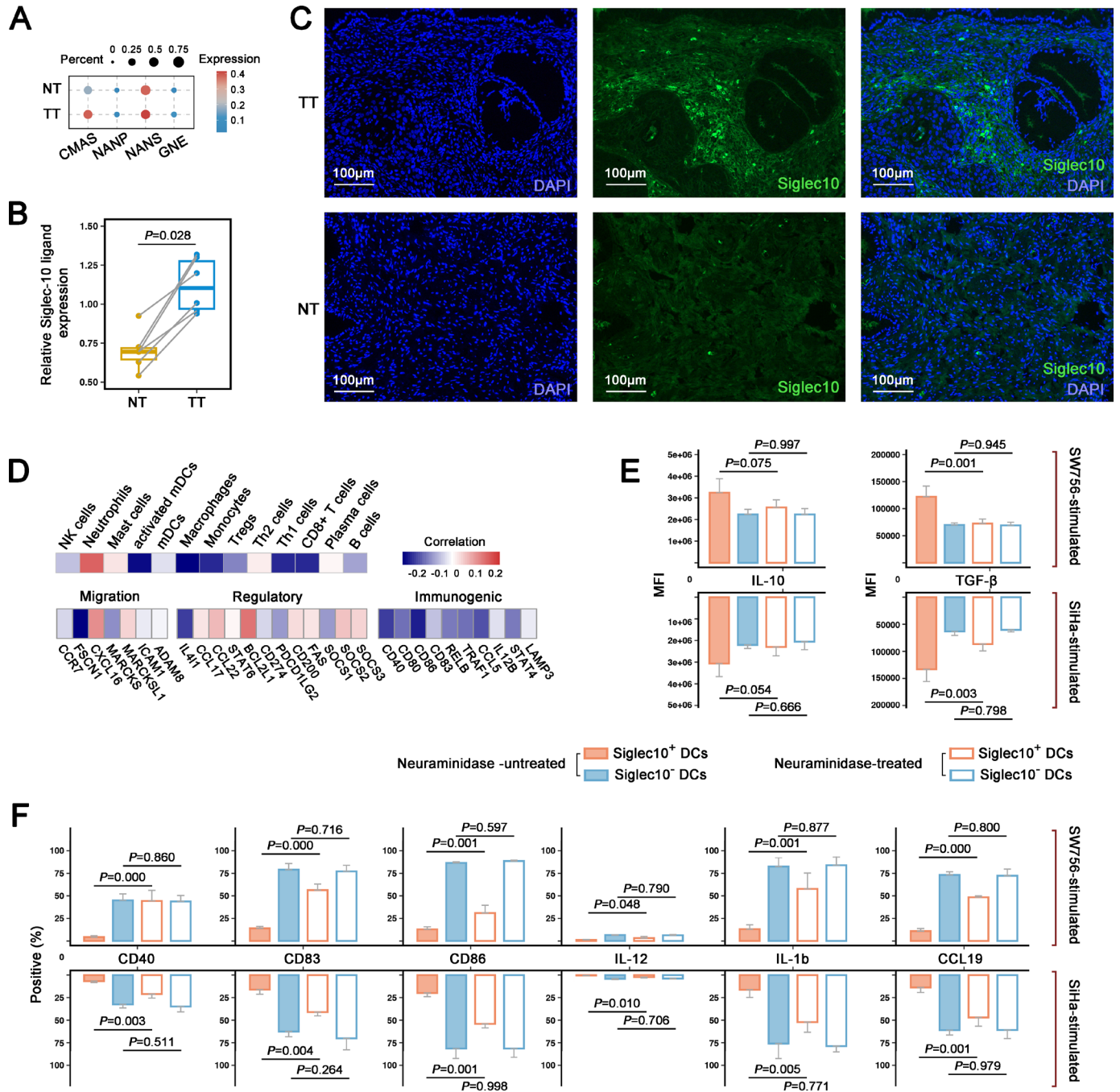


Figure 4 Abundant Siglec-10 ligand signals in cervical cancer predisposed Siglec-10⁺ DCs to a tolerogenic phenotype. (A) Bubble heatmap showing the gene expression of the Siglec family among DCs across the NT and TT samples. (B) Quantification of relative Siglec-10 ligand expression (per DAPI) via immunofluorescence analysis of NT and TT samples (n=6). Three fields on each slide were randomly selected. Significance was calculated by the Wilcoxon matched-pairs signed-ranks test. (C) Representative immunofluorescence staining of Siglec-10 ligands in the NT and TT samples. Tissue sections were processed and stained with antibodies against Siglec-10 ligands and DAPI. (D) Heatmap of the correlation between the sialylation score and immune infiltration score (estimated by CIBERSORT) or the expression of the designated genes in the TCGA CESC data set (n=306). The Spearman rank correlation test was used for the correlations (R: Spearman correlation coefficient). (E) Expression IL-10 and TGF- β in Siglec-10⁺ DCs or Siglec-10⁻ DCs after stimulation with SiHa or SW756 cells (with or without neuraminidase pretreatment), as determined by flow cytometry (n=3). P values were obtained by one-way analysis of variance with the least significant difference test. (F) Expression of designated functional markers in Siglec-10⁺ DCs or Siglec-10⁻ DCs after stimulation with SiHa or SW756 cells (with or without neuraminidase pretreatment) according to flow cytometry analysis (n=3). P values were obtained by one-way analysis of variance with the least significant difference test. CESC, cervical squamous cell carcinoma; DAPI, 4,6-diamidino-2-phenylindole; DC, dendritic cell; IL, interleukin; MFI, mean fluorescence intensity; NT, normal tissue; TCGA, the Cancer Genome Program; TGF, transforming growth factor; TT, tumor tissue.

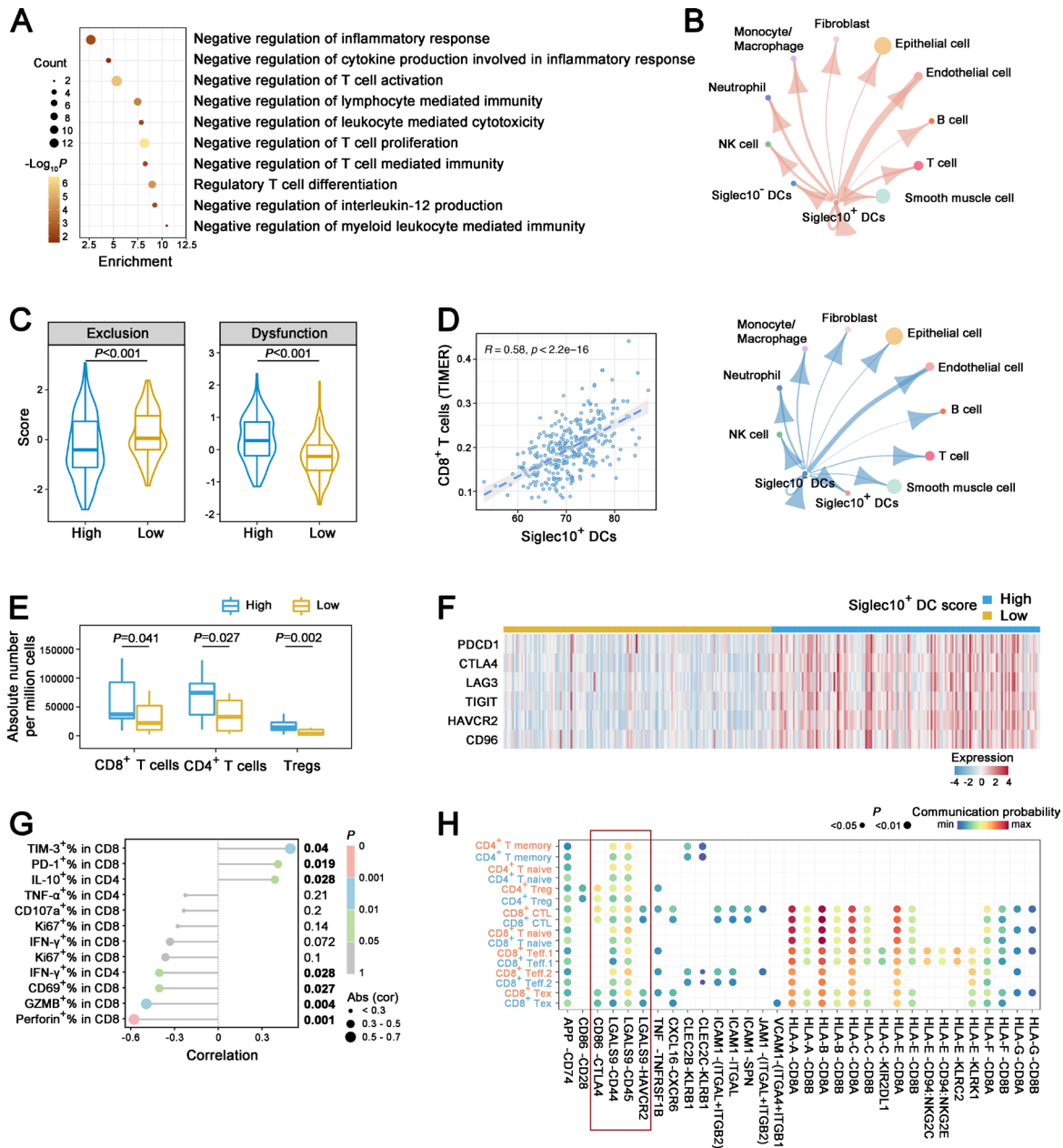


Figure 5 High-intensity-infiltrated Siglec-10⁺ DCs interact with T cells to promote their dysfunction and exhaustion. (A) Enriched Gene Ontology terms in patients with high Siglec-10⁺ DC infiltration in the TCGA-CESC cohort. The infiltration score was calculated according to the gene signature derived from the scRNA-seq data. (B) Network diagram of ligand-receptor interactions between cell populations as determined by CellChat. The width of each solid line is proportional to the interaction weight. Arrows indicate communication from ligand-bearing to receptor-bearing populations. (C) Tumor immune dysfunction and exclusion score across patients with high or low Siglec-10⁺DC infiltration in the TCGA-CESC cohort. The infiltration score was calculated according to the gene signature derived from the scRNA-seq data. Significance was calculated by the Mann-Whitney U test. (D) Correlation between Siglec-10⁺ DC infiltration (calculated according to the gene signature derived from the scRNA-seq data) and CD8⁺ T-cell infiltration (estimated by TIMER) in the TCGA-CESC cohort. The Spearman rank correlation test was used for the correlations. (E) Intratumoral abundance of CD8⁺ T cells, CD4⁺ T cells and Tregs in TT specimens with high or low Siglec-10⁺ DC infiltration, based on flow cytometry analysis (n=31). Significance was calculated by the Mann-Whitney U test. (F) Heatmap showing the differences in the expression of inhibitory receptors between patients with high and low Siglec-10⁺DC infiltration in the TCGA-CESC cohort. The infiltration score was calculated according to the gene signature derived from the scRNA-seq data. (G) Lollipop graph of the correlation between Siglec-10⁺ DC infiltration and functional marker expression in T cells from TT specimens based on flow cytometry analysis (n=31). The Spearman rank correlation test was used for correlations (Abs (cor): Absolute value of the Spearman correlation coefficient). (H) Bubble chart showing significant ligand-receptor pairs between Siglec-10⁺ DCs (indicated in red) or Siglec-10⁻ DCs (indicated in blue) and different T-cell subsets identified by CellChat. CESC, cervical squamous cell carcinoma; DC, dendritic cell; NK, natural killer; scRNA-seq, single-cell RNA sequencing; TCGA, the Cancer Genome Program; TIMER, Tumor Immune Estimation Resource; Treg, regulatory T cells; TT, tumor tissue.

CD4⁺ T cells was also positively correlated with Siglec-10⁺ DC infiltration, and an increase in the Treg number was associated with increased Siglec-10⁺ DC infiltration (online supplemental figure S5B). The results were validated in our patient with CC cohort using flow cytometry analysis, which confirmed that the population with abundant Siglec-10⁺ DCs was characterized by extensive intratumoral T-cell infiltration (figure 5E and online supplemental figure S5C). The expression of a variety of inhibitory receptors (PDCD1, CTLA4, LAG3, TIGIT, HAVCR2, and CD96), which are known to be highly expressed on exhausted T cells, was dramatically greater in the higher-infiltrated TME than in the lower-infiltrated TME (figure 5F). We then examined the functional status of T cells corresponding to different intratumoral Siglec-10⁺ DC levels in our patient with CC cohort. The results showed that Siglec-10⁺ DC infiltration was positively associated with PD-1 and Tim-3 expression in CD8⁺ cytotoxic T lymphocytes (CTLs) as well as IL-10 secretion by CD4⁺ T cells. Conversely, the activation of T cells, as measured by CD69 expression, and the cytolytic capacity of T cells, as determined by granzyme B (GZMB) and perforin expression, were inhibited with increased Siglec-10⁺ DC infiltration (figure 5G). All these observations suggested that Siglec-10⁺ DCs promote immune escape by inducing T-cell dysfunction but not by preventing T-cell infiltration. We further focused on the biologically important interactions between DCs and different T-cell populations to identify the underlying mechanism by which Siglec-10⁺ DCs regulate T-cell function. Both Siglec-10⁺ and Siglec-10⁻ DCs exhibited comparable and abundant interactions with T cells through major histocompatibility complex molecules (figure 5H). In particular, obvious crosstalk between galectin-9 ligands and CD44/CD45/Tim-3 receptors was observed between T-cell subsets and Siglec-10⁺ DCs (figure 5H), which indicated that Siglec-10⁺ DCs might suppress the antitumor function of T cells by upregulating inhibitory galectin-9 signaling.²⁸ Furthermore, Siglec-10⁺ DCs exhibit increased communication with Tregs and CTLs via CD86/CTLA4 coinhibitory signaling.

Blockade of Siglec-10 signaling reinvigorates antitumor immunity by repolarizing DCs

To investigate the therapeutic potential of Siglec-10⁺ DCs as immunotherapy targets for CC, we next investigated whether direct blockade of Siglec-10 by monoclonal antibodies (mAbs) could enhance the DC-mediated antitumor response using PDTF platforms. Annexin V/propidium iodide (PI) staining and flow cytometric analysis revealed that an increased percentage of CC-derived tumor cells treated with the Siglec-10 blocking mAb entered the apoptotic state compared with those treated with the IgG control (figure 6A), and the tumor-killing efficiency was found to be related to the baseline proportion of Siglec-10⁺ DCs before treatment (online supplemental figure S6A). The DC functional state analysis showed that Siglec-10⁺ DCs responded to the Siglec-10

mAb by upregulating CD83 and enhancing inflammatory activity, while Siglec-10⁻ DCs were insensitive to the mAb (figure 6B and online supplemental figure S6B). Furthermore, Siglec-10 blockade augmented the secretion of effector cytokines and cytotoxic granules by CTLs, and this effect was more pronounced in tumors that were treated with the Siglec-10 mAb (figure 6C and online supplemental figure S6C). Due to the expression of Siglec-10 on both DCs and macrophages, we tested the effects of Siglec-10 blockade on tumor cell death after DC depletion to determine which population is responsible for the effective immune response. Despite the presence of macrophages, the therapeutic effect of the Siglec-10 mAb was significantly abrogated in the absence of DCs, indicating that DCs are essential components for effective Siglec-10-targeting therapy (figure 6D). We also found that depletion of CD8⁺ T cells attenuated the antitumor efficacy of Siglec-10 mAb blockade, suggesting that CD8⁺ T cells play a vital role in mediating the blockade of Siglec-10⁺ DCs to elicit tumor inhibition (online supplemental figure S6D).

CD24 is a primary ligand that interacts with Siglec-10, which is overexpressed by multiple tumors, to deliver “do not eat me” signals and prevent immune clearance. The data generated by bulk sequencing and scRNA-seq showed broad upregulation of CD24 expression in cervical tumors but not in adjacent NTs and scarce CD24 expression in other cell types in contrast to that in CC tumor epithelial cells (online supplemental figure S7A,B). Therefore, we sought to investigate whether CD24 is a potential therapeutic target for CC by examining the effect of disrupting CD24-Siglec-10 signaling on DC function using a CD24 mAb. Flow cytometry-based measurements revealed that the tolerogenic activity of Siglec-10⁺ DCs was inhibited by the CD24 mAb compared with that of the IgG control (online supplemental figure S7C), indicating that CD24 is a promising target for further investigation of CC treatment.

Blockade of Siglec-10 enhances the efficacy of anti-PD-1/PD-L1 therapy

According to the abovementioned findings, a positive correlation was observed between Siglec-10⁺ DCs and the expression of PD-1 and between Siglec-10⁺ DCs and the exhaustion of CTLs. Consequently, we proceeded to explore whether the response to the Siglec-10 mAb could be further augmented through concomitant inhibition of PD-1. According to the ex vivo treatment tests conducted with the PDTFs, while the Siglec-10 mAb and PD-1 mAb, which are individual drugs, were able to induce tumor cell death in certain specimens, the combination of these two blockade agents yielded superior efficacy (figure 7A,B). The enhanced therapeutic efficacy of the combination therapy was accompanied by increased CD8⁺ T-cell proliferation and a greater proportion of CTLs expressing CD107a, GZMB, perforin, interferon- γ and tumour necrosis factor- α (TNF- α) (figure 7C,D). These findings suggested that the blockade of Siglec-10 in

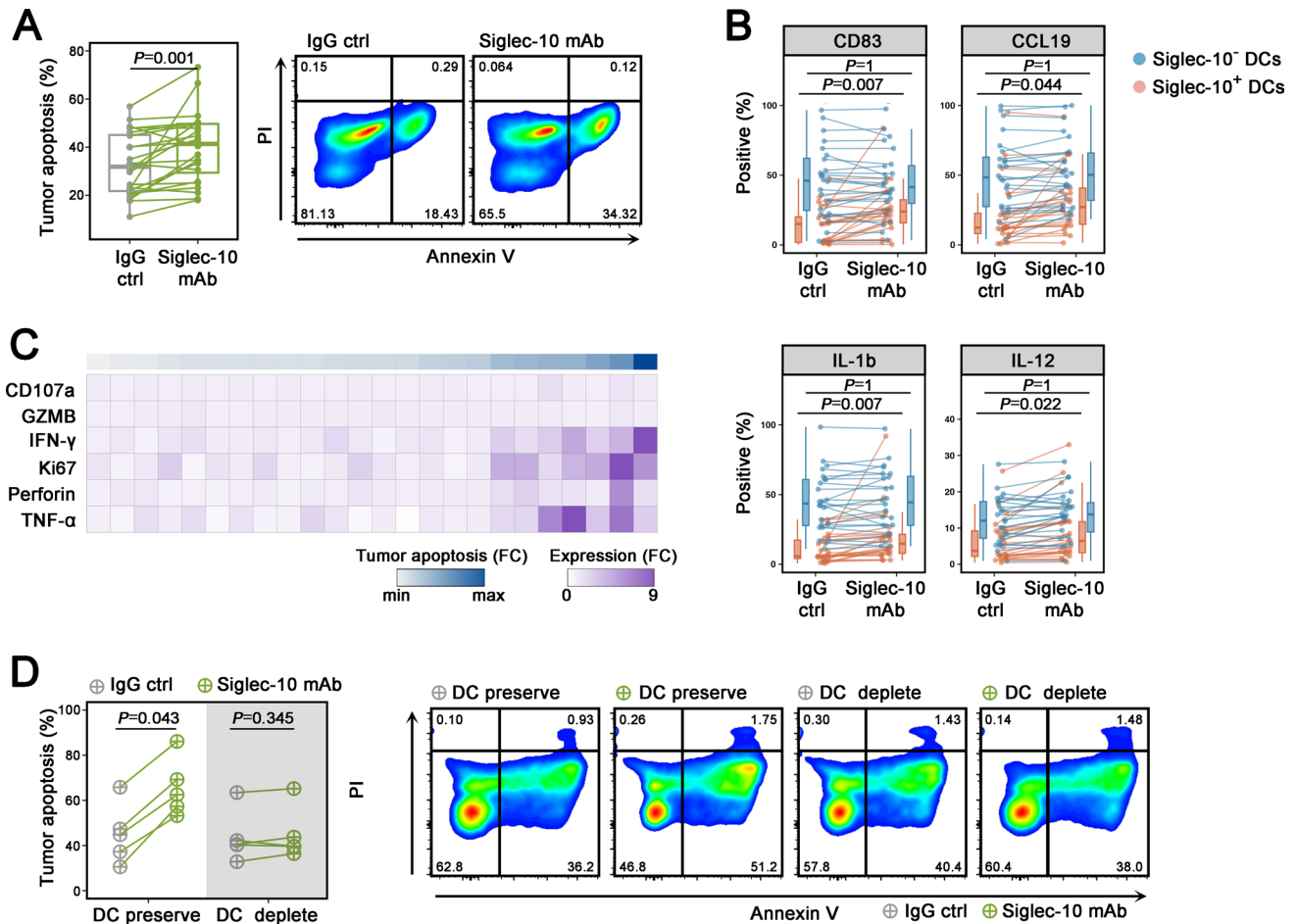


Figure 6 Targeting Siglec-10⁺DCs to elicit antitumor activity. (A) Apoptosis rate of CD45⁻ tumor cells after ex vivo treatment with the anti-Siglec-10 mAb or IgG control for 48 hours, based on flow cytometry analysis (n=24). Apoptosis was measured by annexin V and PI staining and representative pseudocolor plots are shown on the right. Significance was calculated via the Wilcoxon matched-pairs signed-ranks test. (B) Positive expression of functional markers among tumor-infiltrated Siglec-10⁺ DCs or Siglec-10⁻ DCs after ex vivo treatment with the anti-Siglec-10 mAb or IgG control for 48 hours, based on flow cytometry analysis (n=24). Significance was calculated by the Friedman test. (C) Heatmap showing the fold changes in designated marker expression in CD45⁺CD8⁺TILs in the presence of the anti-Siglec-10 mAb compared with that in the presence of the IgG control (n=24). The data are arranged according to the fold change in the apoptosis rate in the presence of the anti-Siglec-10 mAb compared with that in the presence of the IgG control (n=24). The data were obtained via immunostaining and flow cytometry analysis of cells after ex vivo treatment. (D) Apoptosis rate of CD45⁻ tumor cells after ex vivo treatment with the anti-Siglec-10 mAb or IgG control for 48 hours in the presence or absence of DCs (n=5), based on flow cytometry analysis. Representative pseudocolor plots from paired samples are shown on the right. Significance was calculated via the Wilcoxon matched-pairs signed-ranks test. DC, dendritic cell; GZMB, granzyme B; IFN, interferon; mAbs, monoclonal antibodies; PI, propidium iodide; TILs, tumor infiltrating lymphocytes; TNF, tumour necrosis factor.

combination with PD-1 therapy synergistically rejuvenates CTL-mediated tumor killing.

DISCUSSION

The identification and characterization of the heterogeneous phenotypes of tumor-infiltrating DCs and the mechanism by which they acquire a unique regulatory phenotype remain elusive. Interactions between Siglec receptors and sialoglycan ligands have emerged as a promising target for enhancing cancer immunotherapy, supported by extensive preclinical evidence and ongoing clinical trials (NCT03665285, NCT04699123, and NCT05259696) conducted in recent years.¹⁴ This

study revealed the significant contribution of Siglec-10, a member of the Siglec family, in shaping the regulatory functionality of DCs in CC, thereby exerting a profound effect on the malignant potential of CC. Our findings highlight that Siglec-10-expressing DCs participates in the precise regulation of tumor immunosuppression by relaying inhibitory signals from hypersialoglycans on CC cells to effector cells responsible for tumor eradication. Importantly, our results provide valuable insights into the potential of Siglec-10-targeted therapy as a promising approach for CC immunotherapy in the future.

Although several inhibitory Sigslecs have been reported to be expressed by DCs, the understanding of the role of

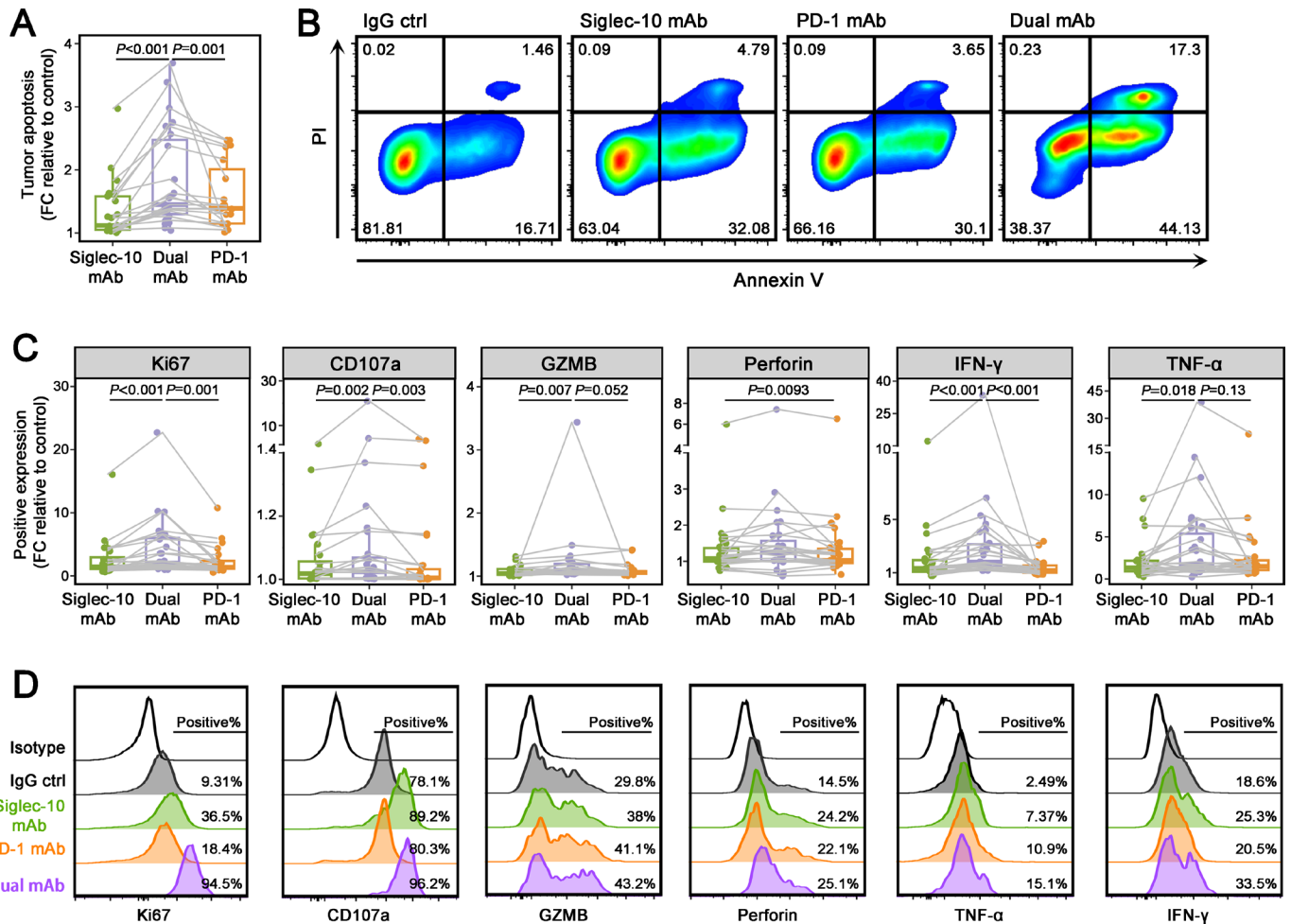


Figure 7 Targeting Siglec-10 to increase the efficacy of anti-PD-1/PD-L1 therapy. (A–B) Fold changes in tumor apoptosis after ex vivo treatment with the anti-Siglec-10 mAb and/or anti-PD-1 mAb compared with that in the IgG control group ($n=24$). Apoptosis was measured by annexin V and PI staining and representative pseudocolor plots are shown. Significance was calculated by the Friedman test. (C–D) Fold changes in designated marker expression in $CD45^+CD8^+$ TILs after ex vivo treatment with the anti-Siglec-10 mAb and/or anti-PD-1 mAb compared with that in the IgG control group ($n=24$). Data were obtained via immunostaining and flow cytometry analysis of cells after ex vivo treatment, and representative histograms are shown. Significance was calculated via the Friedman test. GZMB, granzyme B; IFN, interferon; mAbs, monoclonal antibodies; PD-1, programmed cell death protein-1; PD-L1, programmed death-ligand 1; PI, propidium iodide; TILs, tumor infiltrating lymphocytes; TNF, tumour necrosis factor.

Siglec expression in DCs within the context of cancer is limited. In the study of Wang, higher expression of Siglec-7 and Siglec-9 and moderate expression of Siglec-10 were found in both type-1 and type-2 tumor-infiltrated cDCs in epithelial ovarian cancer, non-small cell lung cancer, and colorectal cancer.²⁹ Here, we found a different expression profile in the CC, and among all of the Siglec members, Siglec-10 was the most highly expressed in CC tumor-infiltrated DCs. Siglec-10 was broadly expressed in the subsets of tumor-infiltrated cDCs but rarely in pDCs. For the first time, we characterized Siglec-10 as an innate immune checkpoint that influences DC function in the TME. Moreover, Siglec-10 initiates the tumor-favoring phenotypic transformation of DCs on receiving intensified sialic acid signaling. The plasticity of DCs during CC formation, growth, and metastasis is gradually enhanced by the upregulation of the Siglec-10 checkpoint and the aberrant sialylation of tumor cells. However, the

specific mechanisms underlying the relationship between Siglec-10 signaling and DC phenotype reprogramming, which may provide new biological insights into the diversity of cell subsets and states within the context of CC, remain to be studied and further verified. Specifically, in contrast to the findings of previous studies reporting a similar ability of mouse splenic SiglecG^{+/+} and SiglecG^{-/-} DCs to internalize OVA, the Siglec-10 checkpoint showed stimulation to the phagocytosis of tumor-infiltrating dendritic cells (TIDCs) from CC.³⁰ This discrepancy is likely due to differences in the innate physiological expression of Siglec-10 and the acquired expression of Siglec-10 under pathological conditions. We hypothesized that the abnormally elevated expression levels of Siglec-10 could induce DC silencing after internalization of the tumor antigen, thus initiating tumor-specific immune tolerance. However, this hypothesis warrants further investigation.



The importance of Siglec-10⁺ DCs in predicting intratumoral CTL function and unfavorable disease outcome underscores the central role of Siglec-10 in suppressing DC activity and facilitating tumor immune escape. The engagement of Siglec-7, Siglec-9 and Siglec-10 by sialoglycans on different tumor cells has recently been demonstrated to induce a cancer-supporting macrophage phenotype by preventing the phagocytosis of cancer cells that induce protective immune responses to the cancer.^{31–34} Blocking Siglec-10 induced the phagocytosis of tumor cells by macrophages and myeloid-derived suppressor cells and synergistically enhanced the response to anti-PD-1 immunotherapy.^{35–36} Previous studies have also revealed that Siglec-7 and Siglec-9 are highly expressed on tumor-infiltrated natural killer and T cells, where they interact with sialoglycan ligands and inhibit tumoricidal activity.^{37–39} The findings from our study, combined with those of previous research, provide robust evidence for the effects of sialoglycan ligand and Siglec receptor interactions on different immune cells. These interactions play an important role in creating an immunosuppressive microenvironment within the context of cancer. Unlike immune cells that directly kill cancer cells, DCs function as shepherds of T cells in cancer by relaying survival or apoptotic signals and driving directional differentiation of T cells, thereby locally modulating antitumor immunity. The identification of enhanced interaction signals involving galectin-9-CD44/CD45/Tim-3 between Siglec-10⁺ DCs and effector CD4⁺ and CD8⁺ T cells provides a potential explanation for the role of this immunoregulatory DC subset in facilitating tumor evasion. Galectin-9 has been reported to transmit signals through CD44 receptors in conjunction with TGF- β signaling, thereby enhancing the stability and function of adaptive regulatory T cells.⁴⁰ Additionally, the binding of galectin-9 ligands to the Tim-3 receptor on T cells has been shown to induce T effector cell inactivation and apoptosis.^{41–42} This study did not provide further clarification on whether the mechanism through which Siglec-10⁺ DCs promote T cell-mediated immunosuppression is dependent on the galectin-9 pathway. Nonetheless, our findings propose new hypotheses regarding how DCs and T cells interact and how immune responses are negatively regulated.

The discovery of barriers to the antitumor function induced by Siglec-10 has shed light on a novel potential target for therapeutic interventions that aim to enhance the antitumor reactivity of both DCs and T cells. The tumor inhibitory effects of Siglec-10 mAb treatment tested in our PDTF models highlight the potential of Siglec-10 intervention for treating CC. The sialoglycan-Siglec axis can be inhibited by either targeting Siglec receptors with antibodies, disrupting sialic acid biosynthesis, or implementing desialylation methods.⁴³ Although there are concerns regarding functional redundancy and potential compensatory mechanisms within the human Siglec repertoire that could potentially dampen the effectiveness of single Siglec-blocking approaches, the potentially

severe adverse events resulting from extensive desialylation of all tissues restrict the applicability of sialic acid interference.^{44–46} It has also been demonstrated that complete abrogation of tumor sialylation can trigger CD8⁺ T cells apoptosis,⁴⁷ which may decrease the efficacy of these approaches. The absence of a consistently and specifically expressed tumor glyco-code in CC poses challenges for the use of cancer cell-targeted desialylation treatment with antibody-sialidase conjugates.¹⁷ Considering the distinctive and notable presence of Siglec-10⁺ DCs in CC, as well as the minimal off-target effects of the Siglec-10 mAb, which necessitates the presence of DCs and T cells for therapeutic response, the inhibition of Siglec-10 is emerging as a potentially effective and moderate approach for disrupting sialoglycan-Siglec signals in CC.

Tumors characterized as “hot” due to the high infiltration of CTLs with signs of T-cell exhaustion have shown increased sensitivity to PD-1/PD-L1 immunotherapy.⁴⁸ Despite the inflammatory nature of most CC tumors, the objective response rate to PD-1 blockade in patients with CC remains less than one-third.⁴⁹ Hence, combining innate and adaptive immunotherapies is highly important, particularly in the context of highly immunogenic but immune checkpoint inhibitor-resistant CCs. Our understanding of the intricate collaboration between DCs and T cells controlled by Siglec-10 and the potential synergistic antitumor immune reactivity of combined treatment with Siglec-10 and PD-1 blockade has pointed toward a new age of combinatorial therapies in the clinical management of patients with CC. To strengthen the evidence, further preclinical experiments using *in vivo* models and safety evaluations must be performed; however, these experiments were not performed in this study due to the unavailability of *in vivo*-grade antibody products. Another unsolved question in our study pertains to the identification of a potential biomarker for treatment with Siglec-10 interfering agents. Clinical studies with large sample sizes are warranted to confirm whether the number of Siglec-10-expressing cells or the density of Siglec-10 ligands could accurately predict immune suppression. Regardless, the exploration of the sialoglycan-Siglec-10 axis has yielded encouraging results in the field of immunotherapy, and the evidence from our study supports further preclinical research and early clinical trials investigating Siglec-10 receptors for CC immunotherapy.

MATERIALS AND METHODS

Patients and specimens

Blood samples from 10 healthy female volunteers (24–32 years old) were collected on written informed consent. Fresh TTs and normal adjacent tissues, as well as peripheral venous bloods were obtained from the Tissue Bank of Obstetrics and Gynecology Hospital, Fudan University. A total of 50 patients pathologically diagnosed with CC by at least two hospital pathologists at the Obstetrics and Gynecology Hospital of Fudan University between March

2021 and September 2022 were enrolled in this study. The detailed data of all patients are provided in online supplemental table S2. All of the samples were anonymously coded (P1-P50), and all of the procedures involving the use of human samples conformed to the guidelines of the Declaration of Helsinki and Tokyo for human experimentation and were approved by the Ethics Committee of the Obstetrics and Gynecology Hospital of Fudan University (2019–123).

Assay methods

The experimental procedures for immunophenotyping of human samples and ex vivo assays with human specimens are described in the supporting information. The detailed methods for flow cytometry and immunostaining are also described in the supporting information. All antibodies used in flow cytometry are listed in online supplemental table S4. The strategy for identifying immune cells is shown in online supplemental figure S2C. For all flow cytometry experiments, we included isotype controls to account for non-specific binding of antibodies. Additionally, untreated cells were used as negative controls to establish baseline fluorescence levels. For immunofluorescence analysis, negative controls were stained with secondary antibodies only (no primary antibodies) to ensure that the observed signals were specific to the primary antibody binding.

scRNA-seq analysis

The scRNA-seq data sets containing information on nine cervical TTs and four paratumor tissues were obtained from the Gene Expression Omnibus Repository (GSE171894 and GSE168652,¹⁸) as well as from Array-Express (accession number E-MTAB-12305¹⁹). Detailed information on the data sets were listed in online supplemental figure S8. The scRNA-seq data sets were processed and filtered using Seurat V.4.3.0 to collect high-quality cells (300–7,000 genes, percentage of mitochondrial genes <10%, percentage of hemoglobin <3%). Before further analysis, the gene expression data was normalized through NormalizeData. The top 3,000 variable genes were scaled and subjected to principal component analysis (PCA) dimensionality reduction. PCA and t-SNE dimension reduction were performed with the top 32 principal components. A nearest-neighbor graph using 32 dimensions of the PCA reduction was calculated using FindNeighbors, followed by clustering using FindClusters with a resolution of 1. Chromosomal copy number variations were inferred from the single-cell gene expression data using the inferCNV (V.1.12.0) R package to classify malignant calls and non-malignant cells. To characterize the cell types in each cluster, we used the automated annotation tool SingleR (V.1.10.0) and manually checked known cell surface markers based on related references. Myeloid cells (approximately 3,299 cells) were extracted for further clustering, ultimately yielding 743 DCs (97 from normal samples and 646 from tumor samples for subsequent analysis).

Statistical analysis

The analysis of single-cell transcriptomic data was performed in R (V.4.0.3). The remaining statistical analyses were performed using IBM SPSS Statistics software (v). The tests used for the statistical analyses are indicated in the legends of each figure. Differences with p values < 0.05 were considered to indicate statistical significance. The values are presented as the means \pm SEMs or medians of biological replicates, as specified.

Contributors YW and Mingxing Zhang initiated the project and designed and supervised the research plan. YW, CW and L-WH performed experiments under the supervision of YW. CW and YW wrote the manuscript. JP, CL and XQ designed and performed the supplementary experiments. Meng Zhang performed statistical analysis. The order of authorship was determined by contribution to the project design and the amount of research performed. All authors edited and approved the manuscript. YW is responsible for the overall content as guarantor.

Funding The authors have not declared a specific grant for this research from any funding agency in the public, commercial or not-for-profit sectors.

Competing interests None declared.

Patient consent for publication Not applicable.

Ethics approval All of the samples were anonymously coded as P1-P35, and all of the procedures involving the use of human samples conformed to the guidelines of the Declaration of Helsinki and Tokyo for human experimentation and were approved by the Ethics Committee of the Obstetrics and Gynecology Hospital of Fudan University (2019-123). Participants gave informed consent to participate in the study before taking part.

Provenance and peer review Not commissioned; externally peer reviewed.

Data availability statement Data are available in a public, open access repository. All data relevant to the study are included in the article or uploaded as supplementary information.

Supplemental material This content has been supplied by the author(s). It has not been vetted by BMJ Publishing Group Limited (BMJ) and may not have been peer-reviewed. Any opinions or recommendations discussed are solely those of the author(s) and are not endorsed by BMJ. BMJ disclaims all liability and responsibility arising from any reliance placed on the content. Where the content includes any translated material, BMJ does not warrant the accuracy and reliability of the translations (including but not limited to local regulations, clinical guidelines, terminology, drug names and drug dosages), and is not responsible for any error and/or omissions arising from translation and adaptation or otherwise.

Open access This is an open access article distributed in accordance with the Creative Commons Attribution Non Commercial (CC BY-NC 4.0) license, which permits others to distribute, remix, adapt, build upon this work non-commercially, and license their derivative works on different terms, provided the original work is properly cited, appropriate credit is given, any changes made indicated, and the use is non-commercial. See <http://creativecommons.org/licenses/by-nc/4.0/>.

ORCID iD

Yumeng Wang <http://orcid.org/0009-0005-6910-6190>

REFERENCES

- Singh D, Vignat J, Lorenzoni V, *et al*. Global estimates of incidence and mortality of cervical cancer in 2020: a baseline analysis of the WHO Global Cervical Cancer Elimination Initiative. *Lancet Glob Health* 2023;11:e197–206.
- Lei J, Ploner A, Elfström KM, *et al*. HPV Vaccination and the Risk of Invasive Cervical Cancer. *N Engl J Med* 2020;383:1340–8.
- Chibwesha CJ, Stringer JSA. Cervical Cancer as a Global Concern: Contributions of the Dual Epidemics of HPV and HIV. *JAMA* 2019;322:1558–60.
- Hayati AR, Zulkarnaen M. An immunohistochemical study of CD1a and CD83-positive infiltrating dendritic cell density in cervical neoplasia. *Int J Gynecol Pathol* 2007;26:83–8.
- Qu X, Wang Y, Jiang Q, *et al*. Interactions of Indoleamine 2,3-dioxygenase-expressing LAMP3⁺ dendritic cells with CD4⁺ regulatory T cells and CD8⁺ exhausted T cells: synergistically

- remodeling of the immunosuppressive microenvironment in cervical cancer and therapeutic implications. *Cancer Commun (Lond)* 2023;43:1207–28.
- 6 Suthen S, Lim CJ, Nguyen PHD, *et al.* Hypoxia-driven immunosuppression by Treg and type-2 conventional dendritic cells in HCC. *Hepatology* 2022;76:1329–44.
 - 7 Huang Z-Y, Shao M-M, Zhang J-C, *et al.* Single-cell analysis of diverse immune phenotypes in malignant pleural effusion. *Nat Commun* 2021;12:6690.
 - 8 Watermann C, Pasternack H, Idel C, *et al.* Recurrent HNSCC Harbor an Immunosuppressive Tumor Immune Microenvironment Suggesting Successful Tumor Immune Evasion. *Clin Cancer Res* 2021;27:632–44.
 - 9 Hinshaw DC, Shevde LA. The Tumor Microenvironment Innately Modulates Cancer Progression. *Cancer Res* 2019;79:4557–66.
 - 10 Demoulin SA, Somja J, Duray A, *et al.* Cervical (pre)neoplastic microenvironment promotes the emergence of tolerogenic dendritic cells via RANKL secretion. *Oncoimmunology* 2015;4:e1008334.
 - 11 Ferns DM, Kema IP, Buist MR, *et al.* Indoleamine-2,3-dioxygenase (IDO) metabolic activity is detrimental for cervical cancer patient survival. *Oncoimmunology* 2015;4:e981457.
 - 12 Barros MR Jr, de Melo CML, Barros MLCMGR, *et al.* Activities of stromal and immune cells in HPV-related cancers. *J Exp Clin Cancer Res* 2018;37:137.
 - 13 Adamik J, Munson PV, Hartmann FJ, *et al.* Distinct metabolic states guide maturation of inflammatory and tolerogenic dendritic cells. *Nat Commun* 2022;13:5184.
 - 14 Stanczak MA, Läubli H. Siglec receptors as new immune checkpoints in cancer. *Mol Aspects Med* 2023;90:101112.
 - 15 Duan S, Paulson JC. Siglecs as Immune Cell Checkpoints in Disease. *Annu Rev Immunol* 2020;38:365–95.
 - 16 Wielgat P, Rogowski K, Niemirowicz-Laskowska K, *et al.* Sialic Acid-Siglec Axis as Molecular Checkpoints Targeting of Immune System: Smart Players in Pathology and Conventional Therapy. *Int J Mol Sci* 2020;21:4361.
 - 17 Rodríguez E, Schetters STT, van Kooyk Y. The tumour glyco-code as a novel immune checkpoint for immunotherapy. *Nat Rev Immunol* 2018;18:204–11.
 - 18 Li C, Guo L, Li S, *et al.* Data from: Single-cell transcriptomics reveals the landscape of intra-tumoral heterogeneity and transcriptional activities of ECs in CC. n.d. Available: <https://doi.org/10.1016/j.omtn.2021.03.017>
 - 19 Li C, Hua K. Data from: Dissecting the single-cell transcriptome network of immune environment underlying cervical premalignant lesion, cervical cancer and metastatic lymph nodes. *ArrayExp* 2023. Available: <https://doi.org/10.3389/fimmu.2022.897366>
 - 20 Cheng S, Li Z, Gao R, *et al.* A pan-cancer single-cell transcriptional atlas of tumor infiltrating myeloid cells. *Cell* 2021;184:792–809.
 - 21 Kim N, Kim HK, Lee K, *et al.* Single-cell RNA sequencing demonstrates the molecular and cellular reprogramming of metastatic lung adenocarcinoma. *Nat Commun* 2020;11:2285.
 - 22 Schneider T, Hoffmann H, Dienemann H, *et al.* Non-small cell lung cancer induces an immunosuppressive phenotype of dendritic cells in tumor microenvironment by upregulating B7-H3. *J Thorac Oncol* 2011;6:1162–8.
 - 23 Jin P, Han TH, Ren J, *et al.* Molecular signatures of maturing dendritic cells: implications for testing the quality of dendritic cell therapies. *J Transl Med* 2010;8:4.
 - 24 Wang Y-M, Qiu J-J, Qu X-Y, *et al.* Accumulation of dysfunctional tumor-infiltrating PD-1+ DCs links PD-1/PD-L1 blockade immunotherapeutic response in cervical cancer. *Oncoimmunology* 2022;11:2034257.
 - 25 Dixon KO, Tabaka M, Schramm MA, *et al.* TIM-3 restrains anti-tumour immunity by regulating inflammasome activation. *Nature New Biol* 2021;595:101–6.
 - 26 Malinarich F, Duan K, Hamid RA, *et al.* High mitochondrial respiration and glycolytic capacity represent a metabolic phenotype of human tolerogenic dendritic cells. *J Immunol* 2015;194:5174–86.
 - 27 Läubli H, Kawanishi K, George Vazhappilly C, *et al.* Tools to study and target the Siglec-sialic acid axis in cancer. *FEBS J* 2021;288:6206–25.
 - 28 Rodrigues Mantuano N, Natoli M, Zippelius A, *et al.* Tumor-associated carbohydrates and immunomodulatory lectins as targets for cancer immunotherapy. *J Immunother Cancer* 2020;8:e001222.
 - 29 Wang J, Manni M, Bärenwaldt A, *et al.* Siglec Receptors Modulate Dendritic Cell Activation and Antigen Presentation to T Cells in Cancer. *Front Cell Dev Biol* 2022;10:828916.
 - 30 Ding Y, Guo Z, Liu Y, *et al.* The lectin Siglec-G inhibits dendritic cell cross-presentation by impairing MHC class I-peptide complex formation. *Nat Immunol* 2016;17:1167–75.
 - 31 Barkal AA, Brewer RE, Markovic M, *et al.* CD24 signalling through macrophage Siglec-10 is a target for cancer immunotherapy. *Nature New Biol* 2019;572:392–6.
 - 32 Mei Y, Wang X, Zhang J, *et al.* Siglec-9 acts as an immune-checkpoint molecule on macrophages in glioblastoma, restricting T-cell priming and immunotherapy response. *Nat Cancer* 2023;4:1273–91.
 - 33 Rodriguez E, Boelaars K, Brown K, *et al.* Sialic acids in pancreatic cancer cells drive tumour-associated macrophage differentiation via the Siglec receptors Siglec-7 and Siglec-9. *Nat Commun* 2021;12:1270.
 - 34 Wang J, Sun J, Liu LN, *et al.* Siglec-15 as an immune suppressor and potential target for normalization cancer immunotherapy. *Nat Med* 2019;25:656–66.
 - 35 Shen W, Shi P, Dong Q, *et al.* Discovery of a novel dual-targeting D-peptide to block CD24/Siglec-10 and PD-1/PD-L1 interaction and synergize with radiotherapy for cancer immunotherapy. *J Immunother Cancer* 2023;11:e007068.
 - 36 Lv K, Sun M, Fang H, *et al.* Targeting myeloid checkpoint Siglec-10 reactivates antitumor immunity and improves anti-programmed cell death 1 efficacy in gastric cancer. *J Immunother Cancer* 2023;11:e007669.
 - 37 Jandus C, Boligan KF, Chijioke O, *et al.* Interactions between Siglec-7/9 receptors and ligands influence NK cell-dependent tumor immunosurveillance. *J Clin Invest* 2014;124:1810–20.
 - 38 Haas Q, Boligan KF, Jandus C, *et al.* Siglec-9 Regulates an Effector Memory CD8⁺ T-cell Subset That Congregates in the Melanoma Tumor Microenvironment. *Cancer Immunol Res* 2019;7:707–18.
 - 39 Stanczak MA, Siddiqui SS, Trefny MP, *et al.* Self-associated molecular patterns mediate cancer immune evasion by engaging Siglecs on T cells. *J Clin Invest* 2018;128:4912–23.
 - 40 Wu C, Thalhamer T, Franca RF, *et al.* Galectin-9-CD44 interaction enhances stability and function of adaptive regulatory T cells. *Immunity* 2014;41:270–82.
 - 41 Zhu C, Anderson AC, Schubart A, *et al.* The Tim-3 ligand galectin-9 negatively regulates T helper type 1 immunity. *Nat Immunol* 2005;6:1245–52.
 - 42 Yang R, Sun L, Li C-F, *et al.* Galectin-9 interacts with PD-1 and TIM-3 to regulate T cell death and is a target for cancer immunotherapy. *Nat Commun* 2021;12:832.
 - 43 Manni M, Läubli H. Targeting glyco-immune checkpoints for cancer therapy. *Expert Opin Biol Ther* 2021;21:1063–71.
 - 44 Schmassmann P, Roux J, Buck A, *et al.* Targeting the Siglec-sialic acid axis promotes antitumor immune responses in preclinical models of glioblastoma. *Sci Transl Med* 2023;15:eadf5302.
 - 45 Gray MA, Stanczak MA, Mantuano NR, *et al.* Targeted glycan degradation potentiates the anticancer immune response in vivo. *Nat Chem Biol* 2020;16:1376–84.
 - 46 Macauley MS, Arlian BM, Rillahan CD, *et al.* Systemic blockade of sialylation in mice with a global inhibitor of sialyltransferases. *J Biol Chem* 2014;289:35149–58.
 - 47 Cornelissen LAM, Blanas A, van der Horst JC, *et al.* Disruption of sialic acid metabolism drives tumor growth by augmenting CD8⁺ T cell apoptosis. *Int J Cancer* 2019;144:2290–302.
 - 48 Morad G, Helmink BA, Sharma P, *et al.* Hallmarks of response, resistance, and toxicity to immune checkpoint blockade. *Cell* 2021;184:5309–37.
 - 49 Monk BJ, Enomoto T, Kast WM, *et al.* Integration of immunotherapy into treatment of cervical cancer: Recent data and ongoing trials. *Cancer Treat Rev* 2022;106:102385.